



OPEN

Improvement of field falling-head test and determination of hydraulic conductivity using Darcy's equation

Bong-Joo Lee

This study presents a novel permeameter design for field falling-head tests to determine vertical hydraulic conductivity (K) using Darcy's equation. The design features an open-ended standpipe with two ports for simultaneous measurement of hydraulic heads at both ends of the sediment column, enabling direct estimation of flow rate (q) and hydraulic gradient (i). Flow rate is calculated by differentiating the best-fit curve for water level change above the sediment, and the hydraulic gradient is derived from the head difference between the ports. Laboratory and field tests consistently demonstrated a strong linear relationship between q and i ($R^2 > 0.999$), validating the applicability of Darcy's equation for this new permeameter design. The K values obtained using the proposed method matched those obtained using the Hvorslev equation method. Furthermore, the design allows for continuous measurement of heads after the falling-head permeameter test, facilitating the collection of time series data for the hydraulic gradient. When combined with a pre-determined K value, this enables calculation of time series for the seepage rate across the surface water/sediment interface. To demonstrate this capability, preliminary tests were conducted using commercially-available pressure transducers to monitor heads and obtain seepage time series. The results of these tests are also presented.

Vertical hydraulic conductivity (K) is a crucial parameter influencing the exchange of water and solutes between surface water and surrounding aquifers¹⁻³. Accurate estimation of K is critical for better understanding interactions between surface water and groundwater systems. Several in-situ approaches have been employed to estimate streambed K , including field permeameter tests³⁻⁵, constant head injection tests⁶, slug tests⁷⁻⁹, grain size analysis¹⁰, and piezo-seep meter¹¹.

Field permeameter tests offer a faster and simpler approach compared to other methods like slug tests and seepage meters. However, conventional permeameter designs, which are essentially hollow cylinders, cannot directly measure the pressure drop across the sediment column. This makes the Darcy equation, which requires both flow rate and hydraulic gradient for K determination, unsuitable for these permeameters.

In contrast, the Hvorslev Equation¹² (Eq. 1) allows K estimation without requiring hydraulic gradient information. This has made it the preferred method for analyzing data from falling-head permeameter tests^{3-5,12-16}.

$$K = \frac{\pi D}{11m} + L \frac{h_0}{t_1 - t_0} \ln \frac{h_0}{h_1} \quad (1)$$

where D is the permeameter diameter, L is the length of the sediment column inside the permeameter, m is the square root of the isotropic ratio of horizontal to vertical hydraulic conductivity, h_0 and h_1 are the water level in the permeameter measured at time t_0 and t_1 . However, the Hvorslev equation relies on the isotropic ratio (m) parameter, which accounts for anisotropy in the sediment and can be challenging to determine accurately in the field. Inaccurate m values can significantly impact K calculations³.

This study proposes a new field permeameter design to address the limitations of conventional permeameters and the Hvorslev equation. The proposed design is an open-ended standpipe permeameter with two ports to measure water levels (heads) at both ends of the sediment column simultaneously. Simultaneous measurements of heads allow for the calculation of both flow rate and hydraulic gradient, enabling K determination using the Darcy equation without consideration of the m value.

This paper describes laboratory and field tests conducted to evaluate the proposed permeameter. The tests assess the linearity between flow rates and hydraulic gradients obtained with the new design. Additionally, the accuracy of the resulting K values is compared to those obtained using the Hvorslev equation method described

Korea Institute of Geoscience and Mineral Resources, Daejeon 34132, South Korea. email: lbj@kigam.re.kr

by Genereux et al.³ (HEM). Finally, the study explores the possibility of obtaining time series for seepage rate by monitoring changes in the hydraulic heads at both ends of the sediment column.

Materials and methods

This study employs a simple permeameter constructed from a stainless-steel standpipe (diameter: 6.3 cm, thickness: 0.1 cm, and length: 120 cm for laboratory test, 150 cm for field test). The standpipe has two ports spaced 60 cm apart: a midsection upper port and a lower port at the base. Flexible tubing (inner diameter: 0.3 cm) connects these ports to a single water level scale, allowing for simultaneous measurement of water levels at both ends (Fig. 1).

After vertical insertion of the permeameter into the sediment bed to a desired depth, water is continuously supplied to the standpipe until excess water overflows from the top. This overflow maintains a constant water level (H_0) above the sediment column inside the standpipe, acting as the upper head for water flow through the sediment. Since the water level (H_0) remains constant, it establishes a constant head (h_0) at the lower end of the sediment column. Following measurement of the constant heads (H_0 and h_0), the water supply is stopped. The water levels, H and h , at both the upper and lower ends of the sediment column are then measured simultaneously at regular time intervals as the permeameter drains, and used to calculate flow rate and hydraulic gradient using Darcy's equation.

The amount of water entering the top of the sediment column (combined flow from the standpipe and tubing) (left hand side of the Eq. 2) must equal the amount of water flow through the sediment column (Darcy's velocity multiplied by the cross-sectional area of the sediment column) (right hand side of the Eq. 2) during the falling-head test¹⁷.

$$(A_s + A_f) \frac{dH}{dt} = -K \frac{\Delta H h}{L} A_s \quad (2)$$

where A_s and A_f = cross-sectional areas of the standpipe and the flexible tubing, $\Delta H h$ = the difference in head between H and h , and L = the length of the sediment column. $\frac{dH}{dt}$ signifies the rate of water level decline above the sediment column. Rearranging of the Eq. 2 leads to the Eq. 3.

$$\left(\frac{A_s + A_f}{A_s} \right) \frac{dH}{dt} = -K \frac{\Delta H h}{L} \quad (3)$$

The left-hand side of Eq. (3) represents the flow rate of water (dH/dt) through the sediment column. This flow rate can be estimated by taking the first derivative of the ExpDec1 function (in OriginPro) for the water level change of H (Eq. 4),

$$y = A_1 \exp(-x/t_1) + y_0 \quad (4)$$

where y , A_1 , x , t_1 and y_0 are water level, amplitude of the decay, elapsed time, time constant and offset, respectively. $\frac{dH}{dt}$ at any given time point (x) is calculated from this derivative and depends on the specific parameters (A_1 , t_1) obtained from the fitted ExpDec1 function. The hydraulic gradient across the sediment column at a given time t is simply obtained by dividing $\Delta H h$ by the length of the sediment column, L . Finally, the vertical hydraulic conductivity, K , can be obtained from the slope of the regression line between flow rate and hydraulic gradient.

Laboratory testing

Figure 1B depicts the laboratory setup for falling-head tests using the new permeameter. A controlled flow environment was achieved with an overflow tank (diameter: 63.5 cm, height: 80 cm) containing layers of 20 cm

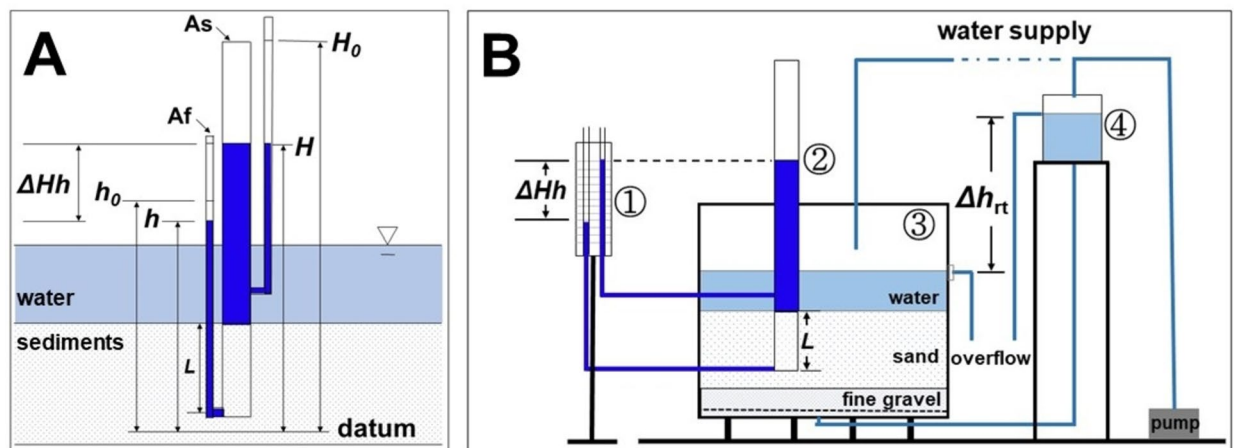


Figure 1. Diagram of the proposed permeameter (A) and experimental setup for laboratory falling-head test (B). ① water level scale, ② permeameter standpipe, ③ overflow sand tank and ④ Constant-head reservoir.

fine gravel and 40 cm sand on top. The permeameter was positioned vertically within the sand bed at a depth of 35 cm. The tank connected to a constant-head reservoir via a 1.6 cm flexible tube. Flow rate and direction of water flow between reservoir and tank were controlled by adjusting a constant head difference (Δh_{rt}) between them. A positive head difference created a constant upward flow (analogous to a gaining stream), while negative values induced a constant downward flow through the sand bed. Δh_{rt} ranged from +46.0 cm to -37.0 cm, with zero Δh_{rt} indicating no flow.

A total of 21 tests were conducted under 7 distinct vertical flow conditions (Δh_{rt}). Before testing, the initial ambient water levels for each Δh_{rt} were recorded for K determination using HEM. Each test under a given Δh_{rt} condition was repeated three times. In all laboratory tests, H_0 is fixed at a constant 60 cm above the tank water level. H and h were measured simultaneously every five minutes for a 25-min test duration. Changes in water level relative to the initial ambient water level were used to calculate K^3 .

As expected as a falling-head test, measured heads (H and h), along with flow rate and hydraulic gradient derived from the heads, exhibited an exponential decrease over time. The rate of decrease varied between tests with different flow conditions (Fig. 2). Difference in decrease rate was attributed to difference in the imposed head above initial ambient water level created under each Δh_{rt} condition. In this study, since target water level, H_0 , was fixed at a constant 60 cm above the tank water level, the imposed head corresponded to the water level difference between target and initial ambient water levels. A lower initial ambient water level led to the larger imposed head, causing a larger driving force for water flow (bottom right panel in Fig. 2). Interestingly, the percentage decrease in flow rates and hydraulic gradients from the beginning to the end of the test (0 to 1500 s) remained consistent across all flow conditions. All tests displayed a very strong correlation ($R^2 > 0.999$) between flow rates and hydraulic gradients. The slopes of these relationships were also consistent across all tests (bottom left panel in Fig. 2). The resulting K values from all tests showed a narrow range with minimal variation (Table 1).

The K values obtained using the permeameter were similar to those obtained using HEM. The percent difference between all K values from both methods was small (average 3.8%). However, slightly larger differences were observed for specific flow conditions: -10.8% at $\Delta h_{rt} = -37.0$ cm and -5.5% at $\Delta h_{rt} = 46.0$ cm. Notably, K values from the proposed method exhibited a normal distribution (Shapiro–Wilk test, p -value = 0.28), while HEM values did not (p -value = 4.4E-4). Despite the non-normal distribution of HEM data, statistical analysis (Kruskal–Wallis ANOVA) showed no significant difference (at the 0.05 level) between the K values obtained from both methods.

Field application in stream and lagoon environments

Falling-head permeameter tests were conducted in sediment beds of the Nosungcheon Stream and Songjiho Lagoon (Fig. 3). The Nosungcheon Stream, a tributary of the Guem River, is approximately 20–30 m wide and 0.3 m deep at the test site in Nonsan city, Korea. The streambed sediment at this location primarily consists of clean, coarse-grained sand. Songjiho Lagoon located on east coast of South Korea is disconnected from seawater

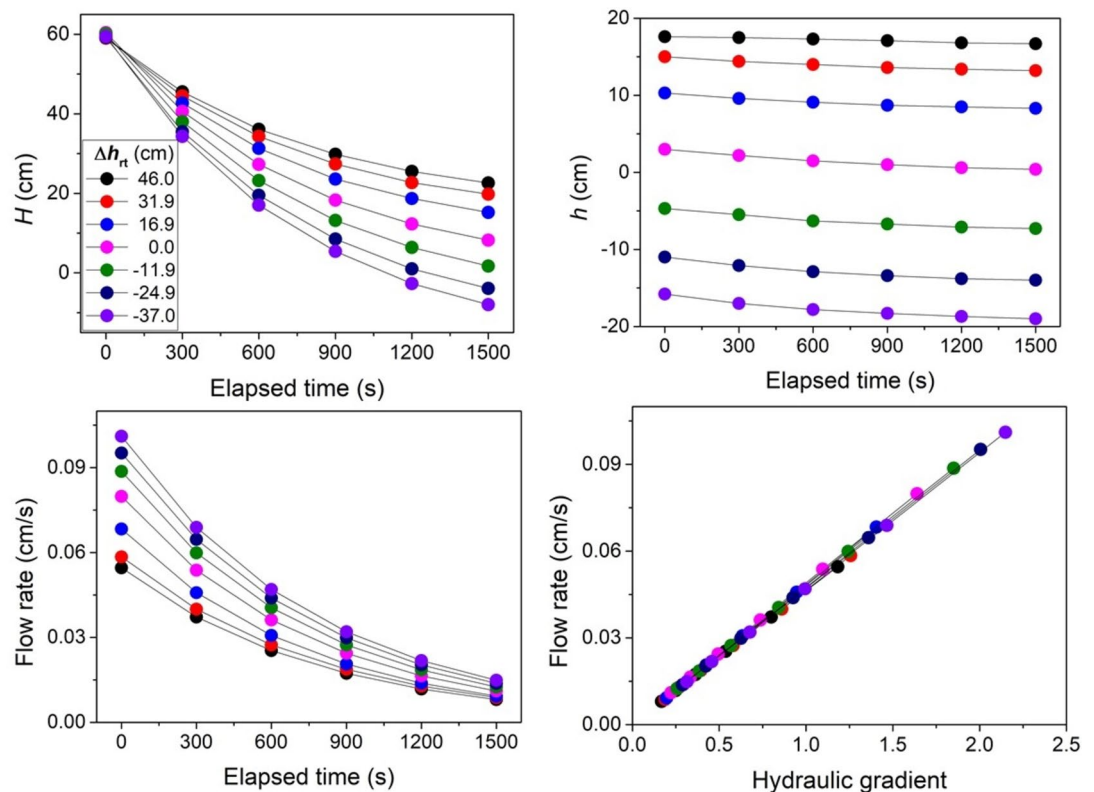


Figure 2. Results of the 1st runs of the laboratory tests under various vertical flow conditions (Δh_{rt}).

Δh_{rt} (cm)	IWL (cm)	IH (cm)	Run	Percentage Decrease (%) of q and i						LR	K (cm/s)		
				q_0	q_{1500}	PD	i_0	i_{1500}	PD	R^2	Proposed	HEM	% D (%)
46	16.8	43.2	1	0.05469	0.00806	85.3	1.18	0.17	85.6	0.99987	0.04592	0.04775	- 3.9
			2	0.05574	0.00801	85.7	1.18	0.17	85.6	0.99998	0.04737	0.04954	- 4.5
			3	0.05533	0.00827	85	1.18	0.17	85.6	0.99987	0.04663	0.05062	- 8.2
31.7	13.1	46.9	1	0.05859	0.00877	85	1.26	0.19	84.9	0.99986	0.04634	0.04631	0.1
			2	0.05999	0.00844	85.9	1.25	0.18	85.6	0.99993	0.04791	0.04631	3.4
			3	0.05987	0.00845	85.9	1.25	0.18	85.6	0.99991	0.04777	0.04631	3.1
16.9	8.1	51.9	1	0.06844	0.00927	86.4	1.4	0.2	85.6	0.99998	0.04893	0.04739	3.2
			2	0.06844	0.00927	86.4	1.4	0.19	86.4	0.99996	0.04893	0.04739	3.2
			3	0.06827	0.00938	86.3	1.4	0.19	86.4	0.99999	0.04845	0.04775	1.5
0	0	60	1	0.08001	0.01107	86.2	1.64	0.22	86.6	0.99997	0.0487	0.04811	1.2
			2	0.07937	0.01118	85.9	1.62	0.22	86.4	0.99999	0.0488	0.04775	2.2
			3	0.07998	0.01097	86.3	1.63	0.23	85.9	0.99998	0.04909	0.04739	3.5
- 11.9	- 7.8	67.8	1	0.08882	0.01253	85.9	1.85	0.26	85.9	0.99997	0.04796	0.04703	2
			2	0.08759	0.0128	85.4	1.85	0.26	86	1	0.04709	0.04667	0.9
			3	0.0887	0.01262	85.8	1.86	0.26	86	0.99998	0.04759	0.04703	1.2
- 25	- 14.5	74.5	1	0.09535	0.0138	85.5	2	0.29	85.5	1	0.04746	0.04631	2.5
			2	0.09486	0.01393	85.3	2.01	0.29	85.6	0.99998	0.04694	0.04631	1.4
			3	0.09457	0.01399	85.2	2.01	0.29	85.6	0.99999	0.04685	0.04631	1.2
- 37	- 16.8	76.8	1	0.1013	0.0149	85.3	2.15	0.31	85.6	0.99999	0.04702	0.05241	- 10.8
			2	0.10072	0.01492	85.2	2.15	0.31	85.6	0.99999	0.04664	0.05205	- 11.0
			3	0.10037	0.01494	85.1	2.14	0.3	86	1	0.04656	0.0517	- 10.5
										Minimum	0.04592	0.04831	
										Maximum	0.04929	0.05241	
										Range	0.00317	0.0061	
										Mean	0.04757	0.04802	3.8
										SD	9.60E-04	2.00E-03	
										CV	2.0	4.2	
										W-statistic	0.94	0.79	
										p	0.28	4.40E-04	

Table 1. Results of the laboratory tests and comparison it to those using HEM. *IWL* initial water level, *IH* imposed head, *PD* percentage decrease, *LR* linear regression, *%D* percent difference, *SD* standard deviation, and *CV* coefficient of variation. Significant words are in bold.

and divided into two sections connected by a deep valley¹⁸. The inner lake connects to an inflowing stream, while the outer lake is separated from the ocean by a sand barrier. While the central area of the lagoon features clayey silt or mud sediments, the areas near the inlet and outlet contain coarse particles¹⁹.

In the Nosungcheon streambed, we performed falling-head tests with the proposed permeameter at four points spaced approximately 4 m apart. Permeameters (Fig. 4A) were inserted vertically 40–60 cm deep using a slide hammer, ensuring an L/D ratio greater than 5. Before testing, the initial ambient water levels in each permeameter were recorded for K determination using HEM. Tests at all four points showed consistent decrease in flow rates and hydraulic gradients, strong linear relationships ($R^2 > 0.999$) between them, and similar regression line slopes (Fig. 5). Comparison to the K values obtained by HEM, the percentage differences in mean K values between the two methods ranged from - 9.3% to 2.3% for the four test points (Table 2), similar to the results observed in the laboratory tests.

In an outlet area of the Songjiho Lagoon, an experiment was performed to obtain time series of the seepage rate using Darcian approach¹³. This involved determining K from falling-head permeameter test, and continuously monitoring the hydraulic heads at both ends of the same sediment column where the falling head test was conducted. Before the tests, the tube connected to the lower port of the permeameter was replaced with a stainless-steel pipe (2.5 cm diameter) (Fig. 4B) to facilitate hydraulic head measurement for obtaining a time series of the seepage rate through continuous head monitoring. The permeameter was inserted 49 cm deep. To account for potential tidal effects on K , falling-head tests were conducted multiple times across the tidal cycle (Fig. 6). The hydraulic heads at the lower end of the sediment column during the tests were measured using electric tape. The resulting K values showed minimal variations, with an average of 0.03982 cm/s, indicating negligible tidal influence. Following the K determination, commercially available pressure transducers were installed in both the permeameter standpipe and 2.5 cm diameter stainless-steel pipe at the lower outlet. Hydraulic heads were continuously monitored every 10 min for a period of 15 days (June 5th to 20th, 2021). Hydraulic gradients were calculated using the head difference (head at lower end - head at upper end) and sediment column length. Heads were also manually measured several times to calibrate the pressure transducer data. After calibration of

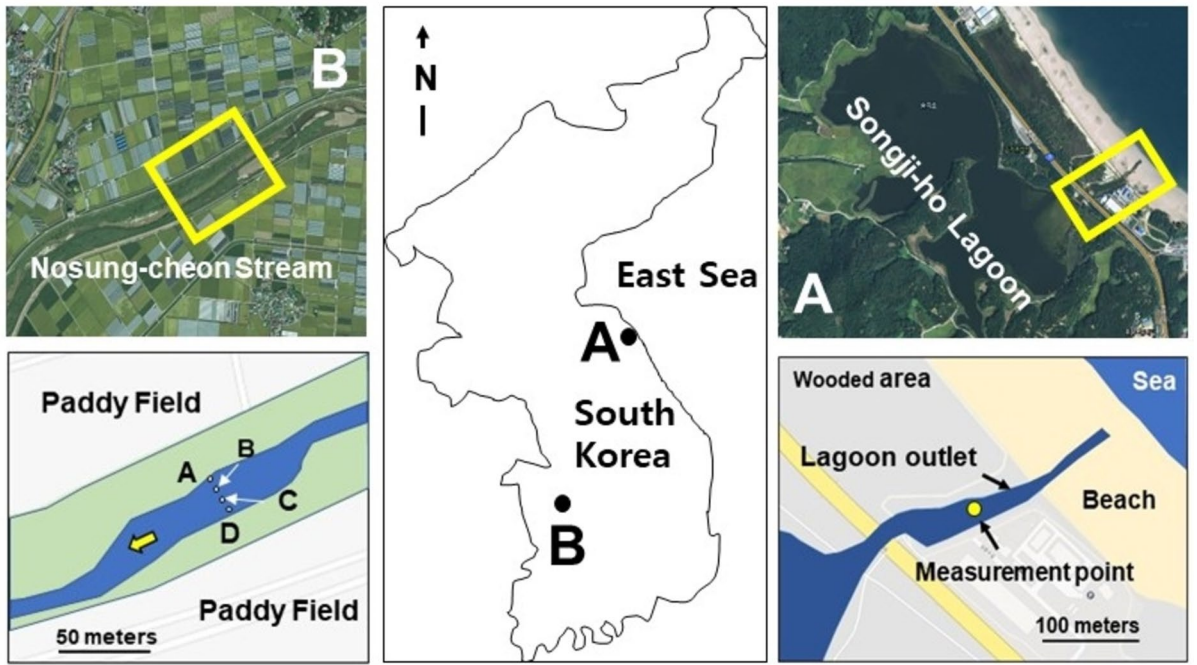


Figure 3. Location maps of test sites. (A): Nosungcheon stream, (B): Songjiho Lagoon. Aerial photos (Kakao Map, downloaded March 31, 2024). Maps were generated with software PowerPoint 2019 <http://www.microsoft.com/>.

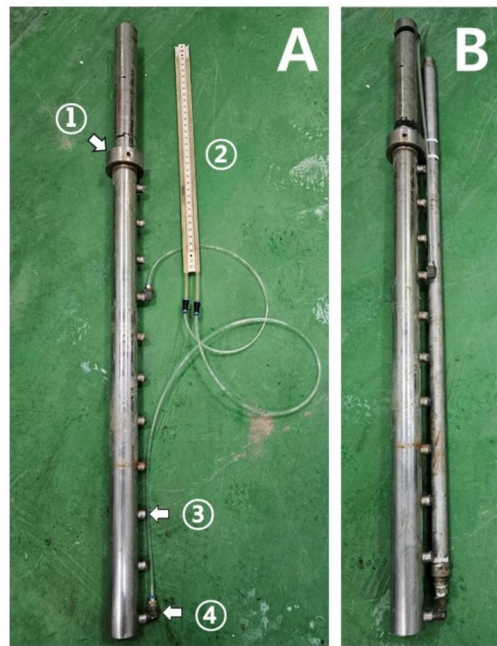


Figure 4. Photos of permeameters used in the field tests. A: permeameter setup for falling-head test for determination of hydraulic conductivity. ① part for slide hammer hitting, ② scale plate to measure hydraulic heads, ③ extra port for tube connection ④ one-touch fit for tube connection. B: setup for monitoring heads after falling-head test. Commercially-available pressure transducers were installed within the permeameter standpipe and the pipe for monitoring heads at double ends of the sediment column which its hydraulic conductivity was determined.

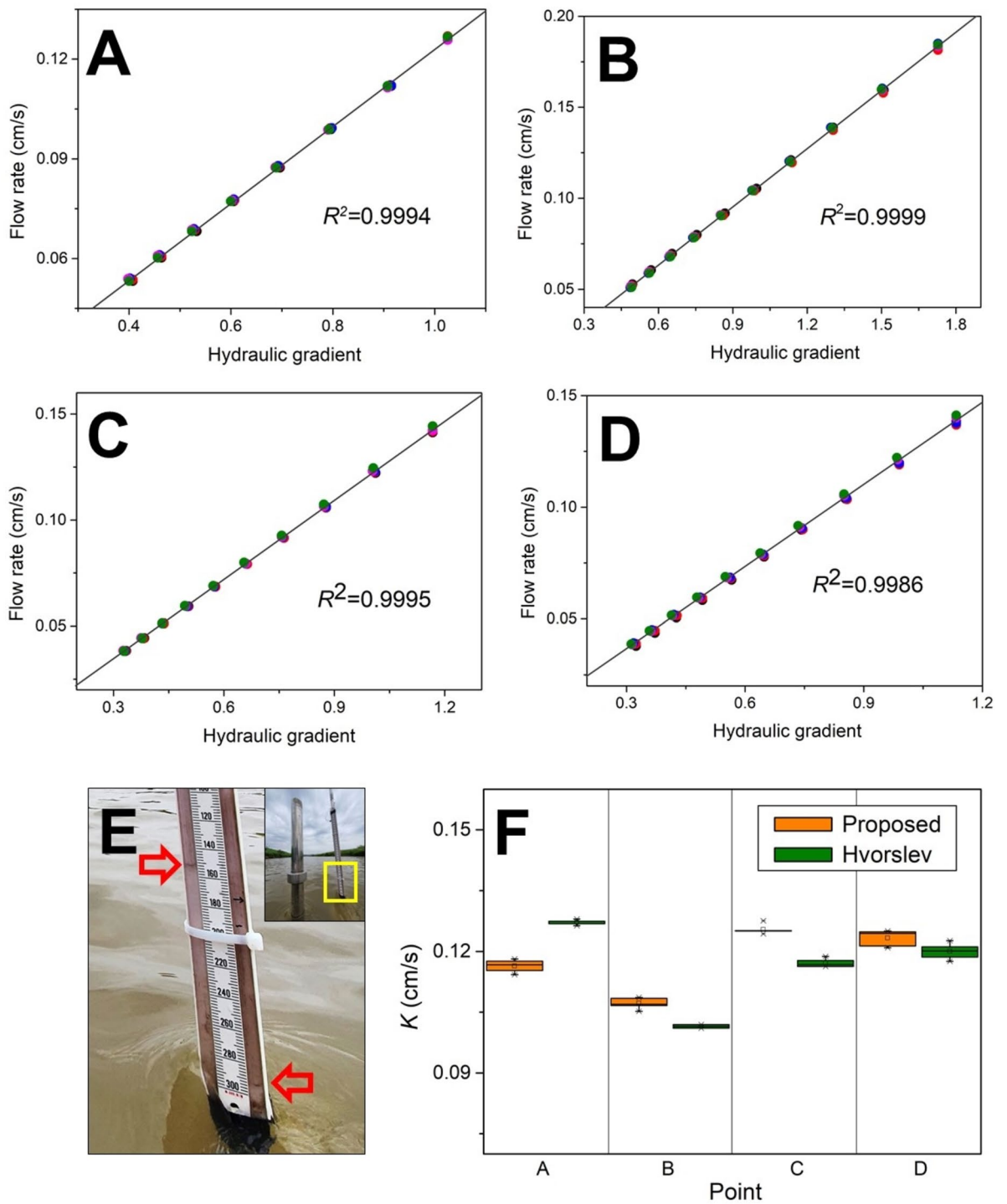


Figure 5. Results of the field tests in a Nosungcheon streambed. (A, B, C, and D): Linear regressions for all pairs of flow rate and hydraulic gradient obtained from the test at each point. (E): Upper and lower water levels in tubes represent the hydraulic heads at upper and lower ends of the sediment column inside the permeameter during falling-head test. (F): Comparisons of the K values obtained by the two methods using box plot.

the pressure transducer data, seepage rates were then determined by multiplying the hydraulic gradients by the average K value obtained from the falling-head permeameter test (Fig. 7). The calculated seepage rates indicated outward flow (lagoon to aquifer) due to higher lagoon water level compared to seawater, and exhibited fluctuations corresponding to the daily tidal cycle (diurnal period), and ranged from 0 to -139 cm/d, with an average seepage rate of -78 cm/d.

Point	Depth (cm)	Run	Percentage Decrease (%) of q and i						LR	K (cm/s)		
			q_0	q_{420}	PD	i_0	i_{420}	PD	R^2	Proposed	HEM	% D (%)
A	55	1	0.1269	0.0533	58	1.03	0.41	60.2	0.99951	0.1173	0.1274	- 8.3
		2	0.1271	0.0537	57.7	1.03	0.41	60.2	0.99962	0.1171	0.1274	- 8.4
		3	0.1268	0.0541	57.3	1.03	0.4	61.2	0.99947	0.1149	0.128	- 10.8
		4	0.126	0.054	57.1	1.03	0.4	61.2	0.99979	0.1139	0.1268	- 10.7
		5	0.1269	0.0533	58	1.03	0.4	61.2	0.99974	0.1163	0.1263	- 8.2
									Range	0.0034	0.0011	
									Mean	0.1159	0.1272	- 9.3
									SD	1.50E-03	6.30E-04	
				q_0	q_{540}	PD	i_0	i_{540}	PD	R^2	Proposed	HEM
B	44	1	0.1813	0.0522	71.2	1.73	0.5	71.1	0.99992	0.1049	0.101	3.8
		2	0.1818	0.0521	71.3	1.73	0.49	71.7	0.99999	0.1048	0.101	3.7
		3	0.1854	0.0511	72.4	1.73	0.49	71.7	0.99998	0.1082	0.1019	6
		4	0.1839	0.0518	71.8	1.73	0.49	71.7	0.99997	0.1065	0.1019	4.4
		5	0.1847	0.0512	72.3	1.73	0.49	71.7	0.99998	0.108	0.1015	6.2
									Range	0.0034	9.00E-04	
									Mean	0.1065	0.1015	4.8
									SD	1.60E-03	4.50E-04	
	C	49	1	0.1415	0.0385	72.8	1.17	0.33	71.8	0.99998	0.1239	0.1163
2			0.1421	0.0383	73	1.17	0.33	71.8	0.99999	0.1245	0.1163	6.8
3			0.1426	0.0383	73.1	1.17	0.33	71.8	0.99998	0.1246	0.1168	6.5
4			0.1426	0.0385	73	1.17	0.33	71.8	0.99991	0.1263	0.1178	7
5			0.1445	0.0382	73.6	1.17	0.33	71.8	0.99993	0.1245	0.1188	4.7
								Range	0.0024	0.0025		
								Mean	0.1248	0.1172	6.3	
								SD	9.00E-04	1.10E-03		
D		50	1	0.1386	0.0379	72.7	1.13	0.32	71.7	0.99994	0.1243	0.1176
	2		0.1371	0.039	71.6	1.13	0.32	71.7	0.99998	0.1208	0.1186	1.8
	3		0.138	0.0393	71.5	1.13	0.32	71.7	0.99996	0.1205	0.1201	0.3
	4		0.1404	0.0386	72.5	1.13	0.31	72.6	0.99997	0.1239	0.1211	2.3
	5		0.1414	0.0388	72.6	1.13	0.31	72.6	0.99997	0.1246	0.1227	1.5
									Range	0.0041	0.0051	
									Mean	0.1228	0.12	2.3
									SD	2.00E-03	2.00E-03	

Table 2. Results of the tests in the Nosungcheon streambed and comparison to those obtained by HEM. PD percentage decrease, LR linear regression, $\%D$ percent difference, SD standard deviation. Significant words are in bold.

Discussion and conclusions

This study proposes a new permeameter design for in-situ falling head tests to determine K using Darcy's equation. Unlike conventional seepage meters, the proposed permeameter directly measures the pressure drop across the sediment column, enabling calculation of flow rate and hydraulic gradient which are required for K determination using Darcy's equation. Laboratory and field tests demonstrated consistent percent decrease in flow rates and hydraulic gradients from the beginning to the end of the test across all flow conditions, confirming accurate head loss measurement by the permeameter. This was further supported by the strong linear relationships between q and i ($R^2 > 0.999$) with very similar regression line slopes, validating the applicability of Darcy's equation for this new permeameter design. Laboratory and field tests also showed that the permeameter produced consistent K values comparable to those obtained by HEM. Percent differences between the two methods in both laboratory and field conditions were less than 11%. These discrepancies were possibly due to inherent differences between the methods, but considered negligible for most practical applications and acceptable for K measurements^{20,21}.

The new permeameter design has several advantages over HEM for K value determination. Unlike HEM, the permeameter leverages Darcy's equation, which doesn't require the isotropic ratio (m). By avoiding m entirely, the new permeameter has the potential for more accurate K determinations. And the new permeameter also doesn't require the initial ambient water level measurement, potentially saving time during field tests. This eliminates a step and simplifies the overall testing process. Additionally, the design facilitates time series collection for the hydraulic gradient and seepage rate, enabling calculations after determining K . Seepage data from the Songjiho Lagoon outlet experiment revealed outward flow (lagoon to seawater) through the aquifer, influenced

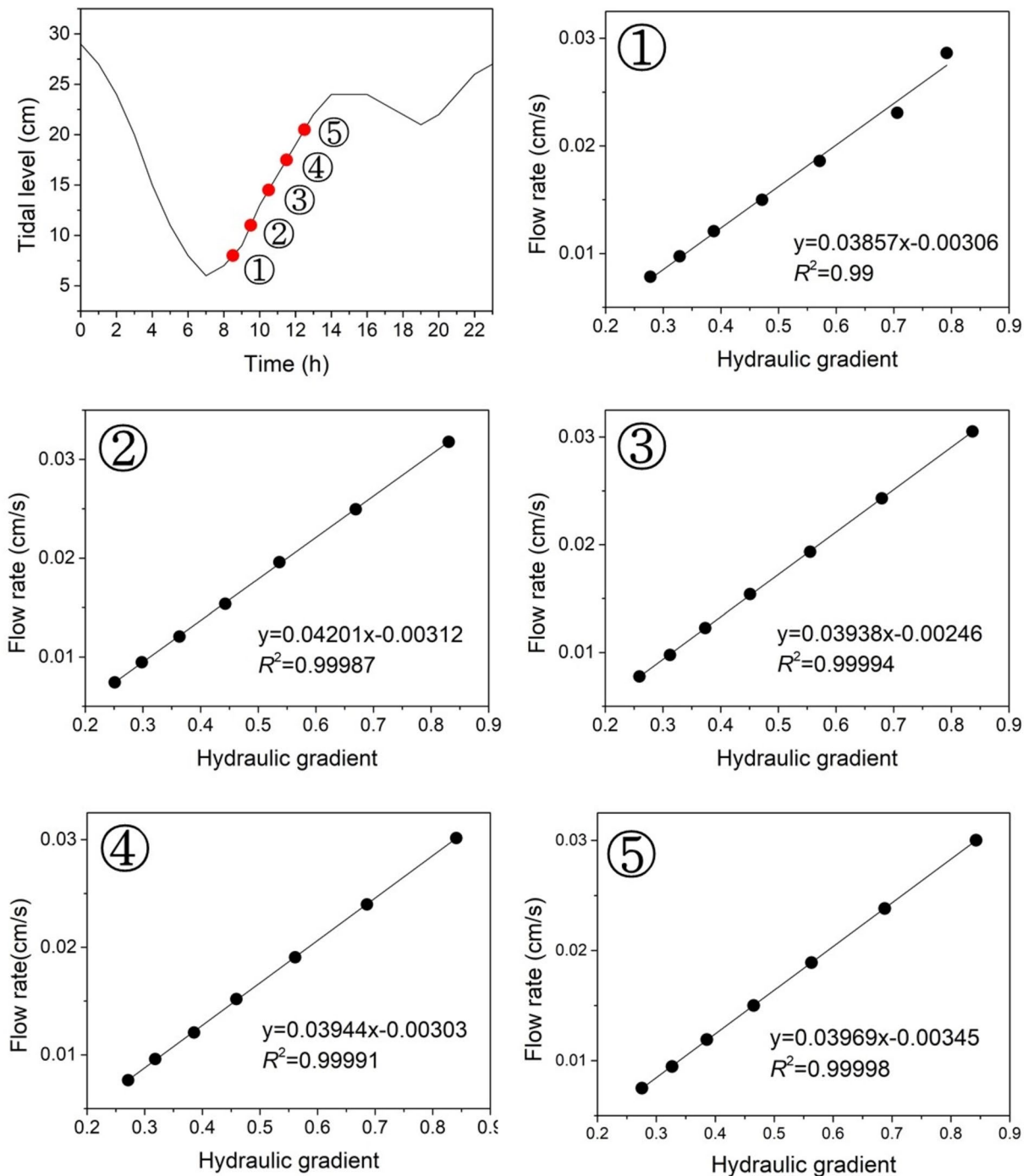


Figure 6. The K values (slopes of the regression lines) determined from the tests conducted multiple times across the tidal cycle at an outlet area of the Songjiho Lagoon.

by tides. The higher lagoon water level creates hydraulic gradients driving this seaward groundwater flow. Tidal fluctuations likely impact the flow rate by affecting the hydraulic gradient. The seepage rates exhibit periodic fluctuations corresponding to the daily tidal cycle (diurnal). Tidal fluctuations of groundwater are common in a coastal aquifer, and the observed sensitivity of seepage rates to these fluctuations suggests the method's potential for studying groundwater-surface water interactions.

The current design of the permeameter might be limited to the top portion of shallow, submerged, soft sediments. Denser sediments like clays or attempts to reach deeper depths might be hindered by clogging or difficulty pushing the permeameter through the sediment. The permeameter requires its top portion to be above the surface water for operation. This can be challenging in locations with deep water or areas experiencing significant water level fluctuations. Simultaneous measurements of water levels at both ends of the sediment column are required. While straightforward under gaining conditions, this becomes challenging in losing conditions (initial ambient

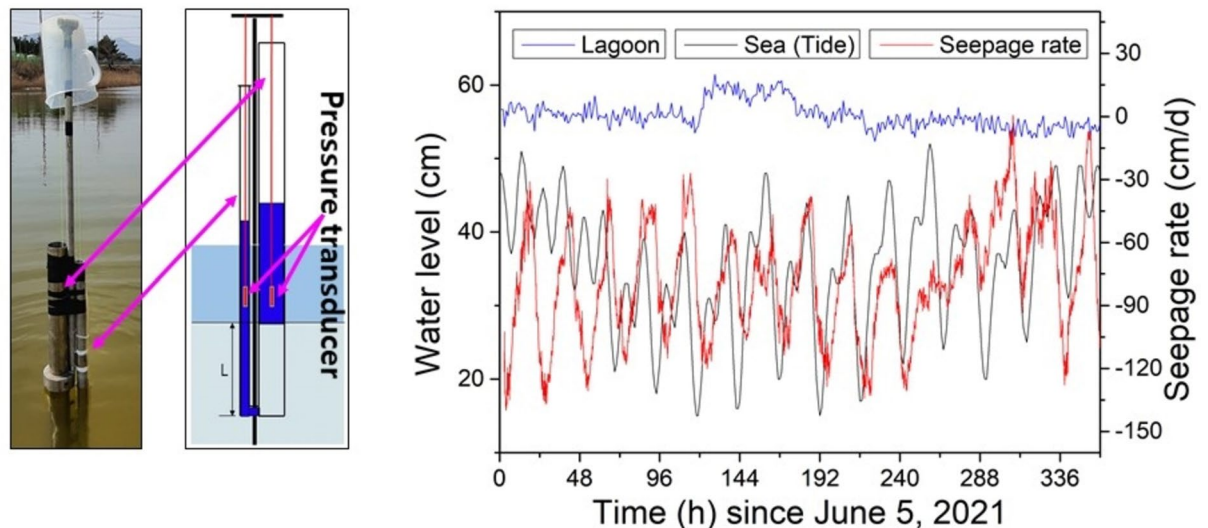


Figure 7. Photo and schematic of the permeameter used to measure heads (left), and the resulting time series of seepage rate (right).

water level is lower than surroundings). Visual observation becomes impractical in such scenarios. Exploring alternative designs or implementing high-accuracy automated water level measuring devices are needed to address these limitations and improve the permeameter's applicability in field investigations.

In conclusion, this new permeameter design offers a valuable tool for determining hydraulic conductivity (K) in-situ using Darcy's equation. It eliminates the need for assumptions about the isotropic ratio and simplifies field testing procedures compared to conventional methods. The ability to collect time series data and its potential for studying groundwater-surface water interactions are additional benefits. Addressing the current limitations related to sediment types, water depth, and water level measurement will further enhance the applicability of this innovative permeameter design.

Data availability

The datasets used and/or analyzed during the current study are available from the corresponding author on reasonable request.

Received: 21 May 2024; Accepted: 29 July 2024

Published online: 02 August 2024

References

1. Saenger, N. *et al.* Numerical study of surface–subsurface exchange processes at a riffle–pool pair in the Lahn River Germany. *Water Resour. Res.* **41**, W12424. <https://doi.org/10.1029/2004WR003875> (2005).
2. Storey, R. G., Howard, K. W. F. & Williams, D. D. Factors controlling riffle-scale hyporheic exchange flows and their seasonal changes in a gaining stream: a three-dimensional groundwater flow model. *Water Resour. Res.* **39**(2), 1034. <https://doi.org/10.1029/2002WR001367> (2003).
3. Genereux, D. P. *et al.* Spatial and temporal variability of streambed hydraulic conductivity in West Bear Creek, North Carolina, USA. *J. Hydrol.* **358**, 332–353. <https://doi.org/10.1016/j.jhydrol.2008.06.017> (2008).
4. Chen, X. Measurement of streambed hydraulic conductivity and its anisotropy. *Environ. Geol.* **39**, 1317–1324. <https://doi.org/10.1007/s002540000172> (2000).
5. Landon, M. K., Rus, D. L. & Harvey, F. E. Comparison of instream methods for measuring hydraulic conductivity in sandy streambeds. *Ground Water* **39**, 870–885. <https://doi.org/10.1111/j.1745-6584.2001.tb02475.x> (2001).
6. Cardenas, M. B., Wilson, J. L. & Zlotnik, V. A. Impact of heterogeneity, bed forms, and stream curvature on subchannel hyporheic exchange. *Water Resour. Res.* **40**, W08307. <https://doi.org/10.1029/2004WR003008> (2004).
7. Cey, E. E., Rudolph, D. L., Parkin, G. W. & Aravena, R. Quantifying groundwater discharge to a small perennial stream in southern Ontario, Canada. *J. Hydrol.* **210**, 21–37. [https://doi.org/10.1016/S0022-1694\(98\)00172-3](https://doi.org/10.1016/S0022-1694(98)00172-3) (1998).
8. Springer, A. E., Petroustou, W. D. & Semmens, B. A. Spatial and temporal variability of hydraulic conductivity in active reattachment bars of the Colorado River Grand Canyon. *Ground Water* **37**(3), 338–344. <https://doi.org/10.1111/j.1745-6584.1999.tb01109.x> (1999).
9. Sebok, E., Duque, C., Engesgaard, P. & Bogh, E. Hydraulic conductivity of streambed sediments of contrasting geomorphological environments. *Hydrol. Process.* **29**, 458–472. <https://doi.org/10.1002/hyp.10170> (2014).
10. Alayamani, M. S. & Sen, Z. Determination of hydraulic conductivity from complete grain-size distribution curves. *Ground Water* **31**(4), 551–555. <https://doi.org/10.1111/j.1745-6584.1993.tb00587.x> (1993).
11. Kelly, S. E. & Murdoch, L. C. Measuring the hydraulic conductivity of shallow submerged sediments. *Ground Water* **41**(4), 431–439. <https://doi.org/10.1111/j.1745-6584.2003.tb02377.x> (2003).
12. Hvorslev, M. J. Time lag and soil permeability in groundwater observations Waterways Experiment Station, Corps of Engineers. *US Army Bull.* **36**, 49 (1951).
13. Kennedy, C. D. *et al.* Comparison of Darcian flux calculations and seepage meter measurements in a sandy streambed in North Carolina, United States. *Water Resour. Res.* **46**, W09501. <https://doi.org/10.1029/2009WR008342> (2010).
14. Dong, W., Chen, X., Wang, Z., Ou, G. & Liu, C. Comparison of vertical hydraulic conductivity in a streambed–point bar system of a gaining stream. *J. Hydrol.* **450–451**, 9–16. <https://doi.org/10.1016/j.jhydrol.2012.05.037> (2012).

15. Burnette, M. C., Genereux, D. P. & Birgand, F. In-situ falling-head test for hydraulic conductivity: Evaluation in layered sediments of an analysis derived for homogenous sediments. *J. Hydrol.* **539**, 319–329. <https://doi.org/10.1016/j.jhydrol.2016.05.030> (2016).
16. Abimbola, O. P. *et al.* Influence of watershed characteristics on streambed hydraulic conductivity across multiple stream orders. *Sci. Rep.* **10**, 3696. <https://doi.org/10.1038/s41598-020-60658-3> (2020).
17. Deming, D. *Introduction to hydrogeology* (McGraw-Hill, 2022).
18. Yum, *et al.* Late Quaternary Environmental Changes of the Hwajinpo and Songjiho Lagoons on the Eastern Coast of Korea. In *Earth Surface Processes and Environmental Changes in East Asia* (ed. Kashiwaya, K.) (Springer, 2015).
19. Sangyong, *et al.* The limnological survey of a coastal lagoon in Korea (4); lake Songji. *Kor. J. Limnol.* **38**(2005), 461–474 (2005).
20. Bagarello, V., Iovino, M. & Elrick, D. E. A simplified falling-head technique for rapid determination of field-saturated hydraulic conductivity. *Soil. Sci. Soc. Am. J.* **68**(1), 66–73. <https://doi.org/10.2136/sssaj2004.6600> (2004).
21. Pedescoll, A., Samsó, R., Romero, E., Puigagut, J. & García, J. Reliability, repeatability and accuracy of the falling head method for hydraulic conductivity measurements under laboratory conditions. *Ecol. Eng.* **37**(5), 754–757. <https://doi.org/10.1016/j.ecoleng.2010.06.032> (2011).

Acknowledgements

This research was supported by the Basic Research Projects (24-3411) of the Korea Institute of Geoscience and Mineral Resources (KIGAM) funded by the Ministry of Science and ICT.

Author contributions

Lee prepared all of the paper.

Competing interests

The author declares no competing interests.

Additional information

Correspondence and requests for materials should be addressed to B.-J.L.

Reprints and permissions information is available at www.nature.com/reprints.

Publisher's note Springer Nature remains neutral with regard to jurisdictional claims in published maps and institutional affiliations.



Open Access This article is licensed under a Creative Commons Attribution-NonCommercial-NoDerivatives 4.0 International License, which permits any non-commercial use, sharing, distribution and reproduction in any medium or format, as long as you give appropriate credit to the original author(s) and the source, provide a link to the Creative Commons licence, and indicate if you modified the licensed material. You do not have permission under this licence to share adapted material derived from this article or parts of it. The images or other third party material in this article are included in the article's Creative Commons licence, unless indicated otherwise in a credit line to the material. If material is not included in the article's Creative Commons licence and your intended use is not permitted by statutory regulation or exceeds the permitted use, you will need to obtain permission directly from the copyright holder. To view a copy of this licence, visit <http://creativecommons.org/licenses/by-nc-nd/4.0/>.

© The Author(s) 2024